STM JOURNALS

Research & Reviews: A Journal of
Pharmaceutical Science

https://journals.stmjournals.com/rrjops

ISSN: 2229-7006
Volume 17, Issue 2, 2026
May–August
DOI (Journal): 10.37591/RRJOPS

Research RRJOPS

Hydrolysis-Driven Optimization of Hydroxypropyl Maize Starch for Improved Micro-Pellet Binding and Quick Solubility of Spirulina-Based Micro-Pellets

Ajay Giripunje[1,*], Srikanth Billa[1], Someshwarnath Pandey[2], Vishnudev Gupta[2], Bishwabhusana Palai[2]

Abstract

Acid hydrolysis is a well-established approach for modifying the physicochemical properties of polysaccharides & macromolecules including hydroxypropyl Maize starch (HPMS). In this study, the effect of varying concentrations of hydrochloric acid on the partial hydrolytic degradation of HPMS (Lycoat RS-780) was investigated at 85°C for 4 h, yielding polymers of different molecular weights. The acid-mediated degradation effects on polymer characteristics were systematically assessed using capillary viscometry and gel permeation chromatography (GPC) to measure molecular weight and distribution. Native & Hydrolyzed Films prepared from the degraded polymers were further evaluated for glass transition temperature, tensile strength, and thermal stability. Additionally, paracetamol-loaded microspheres based on hydroxy propylated maize starch and spirulina extract were produced from hydrolyzed polymer solutions to investigate the impact of degradation on their drug-release profile. The dissolution & disintegration results demonstrated that hydrolytic degradation substantially changed the release kinetics, confirming acid hydrolysis as an effective method for enhancing drug-release rates from HPMS-coated microspheres with spirulina extract compared with HPMC and native starch coatings.

Keywords: Hydroxy propylated maize starch, acid hydrolysis, degradation, spray coating, micro-pellet binding

INTRODUCTION

The use of edible films and coatings has become an essential strategy in the development of pharmaceutical dosage forms, particularly for improving product stability, protecting active pharmaceutical ingredients (APIs), and modulating drug release characteristics. Edible coating systems are generally classified into three major categories: lipids (such as waxes and fatty acids), hydrocolloids (including polysaccharides and proteins), and composite materials derived from their combinations. Among these, hydrocolloid-based materials, especially polysaccharides, have gained considerable interest due to their excellent film-forming ability, biocompatibility, and favorable barrier properties against oxygen and other environmental factors. However, the presence of hydrophilic functional groups in polysaccharide chains often leads to moisture absorption under ambient conditions, which may influence the mechanical integrity and barrier performance of the resulting films.

Among the wide range of polysaccharides available for pharmaceutical and biomedical

***Author for Correspondence**
Ajay Giripunje
E-mail: ajay.giripunje@gmail.com

[1]ACG Associated Capsules Pvt Ltd, Mumbai, Maharashtra, India
[2]Professor, Department of Chemistry, SJJT University, Jhunjhunu, Rajasthan, India

Received Date: March 27, 2026
Accepted Date: April 28, 2026
Published Date: May 02, 2026

Citation: Ajay Giripunje, Srikanth Billa, Someshwarnath Pandey, Vishnudev Gupta, Bishwabhusana Palai. Hydrolysis-Driven Optimization of Hydroxypropyl Maize Starch for Improved Micro-Pellet Binding and Quick Solubility of Spirulina-Based Micro-Pellets. Research & Reviews: A Journal of Pharmaceutical Science. 2026; 17(2): 41–61p.

© STM Journals 2026. All Rights Reserved

applications, maize starch has emerged as one of the most promising natural polymers owing to its abundance, biodegradability, and economic viability. Starch is the second most abundant natural polysaccharide after cellulose and represents a renewable resource that is widely distributed in cereal grains, tubers, and legumes. Chemically, starch is composed of two structurally distinct glucose polymers: amylose, which is primarily a linear α-(1→4)-linked glucan, and amylopectin, a highly branched polymer containing both α-(1→4) and α-(1→6) glycosidic linkages. The relative proportion and molecular organization of amylose and amylopectin strongly influence the physicochemical, rheological, and functional properties of starch, including gelatinization behavior, viscosity development, and film-forming capability (Tharanathan, 2003; Singh et al., 2003).

Maize starch is obtained from the endosperm of *Zea mays* and typically appears as a white, odorless, and tasteless powder composed of semicrystalline granules. When dispersed in water and subjected to heat, starch granules undergo a process known as gelatinization, during which the crystalline regions of the granule are disrupted, leading to swelling, hydration, and eventual release of amylose molecules into the surrounding medium. This process results in the formation of a viscous paste that can subsequently form continuous polymeric films upon drying. The ability of gelatinized starch to produce transparent and flexible films, particularly in the presence of plasticizers, such as glycerol or sorbitol, has attracted significant attention for applications in biodegradable packaging, edible coatings, and pharmaceutical delivery systems (Liu et al., 2008; Avérous, 2004).

In pharmaceutical formulations, starch and its derivatives have long been used as multifunctional excipients, serving as binders, disintegrants, fillers, matrix-forming agents, and coating materials in a wide range of dosage forms. Their natural origin, biocompatibility, and low toxicity have further supported their acceptance in pharmaceutical and biomedical applications. In recent years, the increasing emphasis on sustainable and environmentally friendly materials has stimulated renewed interest in starch-based polymers as alternatives to synthetic excipients for film coating and controlled drug delivery systems (Rowe et al., 2009).

Despite these advantages, the direct application of native starch in advanced pharmaceutical coatings and film systems is often limited by certain inherent drawbacks. Native starch typically exhibits relatively high viscosity, poor mechanical strength, and sensitivity to moisture, which may compromise its performance in industrial processing and product stability. These limitations are closely associated with the molecular weight distribution, branching architecture, and supramolecular organization of amylose and amylopectin molecules within the starch granule. Consequently, modification or controlled degradation of starch polymers has become an important strategy to tailor their physicochemical and functional properties for specific applications (Hoover, 2000).

Understanding the relationship between polymer molecular weight and formulation performance is, therefore, crucial for the rational design of starch-based pharmaceutical materials. Variations in molecular weight can significantly affect rheological behavior, gel strength, film flexibility, and drug release characteristics. For instance, Mali et al. demonstrated that controlled reduction in starch molecular weight resulted in improved flexibility and reduced brittleness of starch-based biodegradable films. Similarly, Lawal and Adebowale reported that structural modification and depolymerization of starch could substantially alter viscosity profiles, swelling capacity, and hydration behavior, thereby influencing its functionality in pharmaceutical formulations.

Several approaches have been explored to modify the molecular structure of starch polymers, including thermal treatment, enzymatic hydrolysis, acid hydrolysis, ultrasonic degradation, oxidation, and radiation-induced depolymerization. Among these techniques, acid hydrolysis remains one of the most widely employed and industrially feasible methods for reducing starch molecular weight in a controlled manner. During acid hydrolysis, glycosidic linkages within amylose and amylopectin chains are selectively cleaved, producing shorter polymer chains and partially hydrolyzed starch fragments. This depolymerization process can significantly alter the physicochemical properties of starch,

© STM Journals 2026. All Rights Reserved

including viscosity reduction, improved solubility, modified gelatinization behavior, and enhanced processability for film formation (Singh et al., 2003; Hoover, 2000).

Traditionally, the characterization of starch-based excipients in pharmaceutical applications has relied heavily on viscosity measurements, which provide a convenient indicator of polymer behavior in solution. However, viscosity measurements alone represent only an averaged macroscopic property and may not adequately capture variations in molecular weight distribution or structural heterogeneity within the polymer matrix. With the growing adoption of Quality by Design (QbD) principles in pharmaceutical development, there is an increasing need for deeper understanding of excipient properties, including molecular structure, thermal behavior, and rheological performance, to ensure consistent product quality and performance (IPEC, 2017).

In this context, the controlled depolymerization of maize starch offers a promising approach for generating polymer fractions with tailored molecular weights and functional characteristics. Such modifications can potentially improve film-forming properties, reduce viscosity-related processing limitations, and enhance the applicability of starch-based materials in pharmaceutical coating systems.

In the present study, we report a facile acid hydrolysis method for the controlled degradation of pharmaceutical-grade maize starch to produce lower molecular weight polymer fractions. The hydrolyzed starch samples were subsequently processed into thermoplastic films and systematically evaluated for changes in their thermal, mechanical, rheological, and solubility properties. Furthermore, drug-loaded microspheres were prepared to investigate the functional implications of starch depolymerization on coating performance and drug release behavior.

To the best of our knowledge, this work provides one of the first comprehensive investigations into the physicochemical and functional characteristics of hydrolyzed maize starch films for pharmaceutical coating applications, offering new insights into the rational design and tailoring of natural polysaccharide-based excipients for advanced drug delivery systems.

EXPERIMENTAL DETAILS

Materials

Hydroxy-propyl Maize starch (HPS Maize starch, (Lycoat RS780) (Hydroxy propyl content HP content 05–08%, Moisture content 5–8%, Residue >500 micron/35 US STD % – 0.5%, Residue on 40 micron – 100%, Iron <10 mg/kg, Silicon dioxide 5 mg/kg, sulphated ash 0.30 %, Total aerobic microbial count <10 cfu/gm, Total yeast and mould count <10 cfu/gm was obtained from Roquette (France). HPLC Water (99.99 % (Supelco), Hydrochloric acid (36%), Sigma Aldrich, USA. Sodium Hydroxide (99%), Sigma Aldrich, USA, Spirulina extract Signet Chemicals, Paracetamol, Glucose Beads and Absolute Ethanol obtained from MEB pharma, India.

Synthesis of Hydrolyzed HPS Maize Starch (Hy-HPMS) Films

To synthesize Hy-HPMS, 40 g of HPMS powder (wt.%/vol) was dispersed in a single-neck 500 mL round-bottom borosilicate glass flask containing 60 mL of preheated (25°C) deionized water. The mixture was continuously stirred for 30 minutes to allow uniform dispersion. Subsequently, concentrated hydrochloric acid was added in varying amounts (0–0.75%, w/w relative to the HPMS powder) for acid hydrolysis, Reaction mixture heated at temperature (85°C) and the reaction mixture was stirred for an additional 4 hours on the 85°C temperature. After the hydrolysis, the reaction mixture was allowed to cool to room temperature. During the cooling process, the solution transitioned from a light hazy white suspension to a clear yellowish, amber-colored solution confirms the transformation of partially hydrated form to fully hydrated and disentangled HPMS solution. To eliminate residual acid and prevent further reaction, the solution was neutralized by the gradual addition of 1% sodium hydroxide solution to pH 6.5 to 7.0. The resulting neutralized, Native & hydrolyzed HPMS (*Hy*-HPMS) solution was further used for film casting.

© STM Journals 2026. All Rights Reserved

Film Casting

The solution obtained from the above process was degassed using a vacuum chamber at 35 °C for 40 minutes. Subsequently, 300 µm films of each composition were cast onto glass plates using a semi-automatic film applicator. The films were then dried on glass plates in a humidity-controlled chamber at 23°C and 55% relative humidity (RH) for 15 hours. The final moisture content of the films was maintained at 14–15%. The films were designated as *Native, Hy-HPMS I, Hy-HPMS II*, and *Hy-HPMS III*, respectively, to the amount of concentrated HCl used for hydrolyzing the HPMS solution.

For 0% HCl: Native, 0.25% HCl: Hy-HPMS II, 0.50% HCl: Hy-HPMS-II, 0.75% HCL: Hy-HPMS III, respectively.

Preparation of Native & Hy-HPMS-Paracetamol Spray Coated Microspheres with Spirulina Extract Color

To evaluate, the different degrees of HPMS hydrolysis influence the drug release profile of the paracetamol drug. Four sets of Native & Hy-HPMS and paracetamol-based spray coated microspheres were prepared as per the procedure described below:

A patented ACG GPCG 1.1 mini spray coater (India) was employed for the spray coating process. Initially, sugar spheres (non-pareil seeds, *20/22 µm*) were sourced from MEB Pharma Supplier Pvt. Ltd. (India). A quantity of approximately *200 g* of sugar spheres was used for the trial, with all calculations referenced to the weight of the sugar beads. Prior to coating, the designed spray coater parameters were set as follows: temperature at *40°C*, atomizing air pressure at *1.2* bar, blower drying speed at *58%*, air flow at *30* cfm, spray pump speed at *4* rpm, spray rate at *4* g/min, and rotor disc motor speed at *280* rpm. Maintaining the above conditions three consecutive layers of coating were applied to the sugar spheres, a *10* % (w/w) HPMS solution (*12.5 g of 40%* prepared HPMS solution dilute in *100* ml DM water was sprayed to form the initial coating layer. *20 % (w/w)* Paracetamol (*40* g) was suspended in *1600* ml of ethanol along with *20* ml of HPMS solution. This mixture was applied as a drug-loaded layer. The final coating layer comprised *25% (w/w) 62.5* g of HPMS solution dissolved in *250* ml of water, to which *16* g of spirulina extract (*8*% w/w) was added, dispersed in *300* ml of HPMS solution. The spirulina extract was added to improve the blue coloration. To prevent moisture uptake, the coated pellets were immediately sealed in airtight containers. The product yield was calculated as the ratio of the dried mass of solids collected to the mass in feed solution. Three replicates were carried out for each treatment for repeatability.

CHARACTERIZATION OF HY-HPMS FILMS

LOD Test

To investigate the effect of hydrolysis degree on residual moisture content in HPMS films, loss-on-drying tests were performed. Each sample (1 g, A1) was weighed and transferred to a clean, dry, pre-weighed glass moisture dish. The dishes were placed in a hot-air oven set at 110 ± 2°C and dried for 6 hours, or until constant mass was reached. Following drying, the samples were cooled in a desiccator containing silica gel for 40 minutes to prevent atmospheric moisture uptake. The dried samples were then reweighed (A2), and the loss of moisture content in percentage (LOD) was calculated using the following formula:

$$Moisture\ Content\ (\%) = \frac{A1-A2}{A1} \times 100. \quad (1)$$

Dynamic Vapor Sorption (DVS)

The water vapor sorption and desorption isotherms from the untreated and treated HPMS films were measured at *27°C* on the DVS Intrinsic Plus, (*Surface Measurements, UK*). Prior to the testing each film was dried and weighed exactly 100 mg was placed into the platinum pan of the DVS. The sample was subjected to the cyclic variation in RH from *0–95%* and then *95 to 0%* in various intervals. The change in mass (%) vs Target % P/Po were recorded and further analyzed.

© STM Journals 2026. All Rights Reserved

Tensile Test

The tensile properties of the as prepared *Hy-HPMS* films were evaluated by using *Shimadzu (Japan) EZ-LX 1KN UTM*. For testing, the films of the *Hy-HPMS* were cut in to dimensions; *length =70 mm × width = 20 mm × thickness = 100 µm*. Prior to the testing, the samples were conditioned at relative humidity (RH) *55% for 24 hours at 23°C* in the humidity chamber which ensures the moisture content of the films is around *15%*. After conditioning, the samples were immediately tested, maintaining a crosshead speed of *2 mm/min with gauge length of 50 mm*. For the sake of reproducibility of the data 7–8 samples of respective *Native & Hy-HPMS films* were tested to produce *stress vs strain* profiles and from the obtained graphs *break strength, break strain and toughness* were recorded.

Fourier Transform Infrared Spectroscopy (FTIR) Studies

The functionality of the respective *Hy-HPMS* films was analyzed spectroscopically in reflectance mode using *PerkinElmer (USA), FTIR (Spectrum-Two) spectrometer*. The Hy-HPMS films were examined in FTIR equipped with attenuated total reflectance (ATR) accessory mounted with Zinc-Selenide crystal window. In the reflectance mode of measurements each sample scanned 128 times between *400–4000 cm^{-1}* with resolution *of 4 cm^{-1}* to record the spectrum. The obtained spectra were further analyzed using *Pyris software IR-ES version 10.7.2.*

Differential Scanning Calorimeter (DSC)

DSC measurements of the Native & *Hy-HPMS* films were performed using *PerkinElmer DSC 4000 (USA)* equipment. The sample weighed between *6–8 mg* sealed in the *50 µl* Aluminum container using crimper press. The sealed sample is subjected to the temperature scan from *25°C to 200°C at a heating rate if 5°C min^{-1}* under inert environment against the sealed empty reference pan. The calibration of the instrument was done using Sapphire standard under same conditions. The heat flow data obtained from the test was further analyzed using the *Pyris software*.

Thermogravimetric analysis (TGA)

The degradation characteristics of the as prepared films were probed using the *PerkinElmer TGA 8000 instrument*. A finely cut film piece weighed between *5–6 mg* placed in the platinum pan and subjected to heating from *30 to 800°C* at rate *of 20°C* min^{-1} in Nitrogen environment. During the analysis the change in the sample weight with respect to the temperature was recorded and further analyzed to obtain the plots of *Wt.% Vs T.*

Capillary Viscometry

The Viscosity average molecular weight *(M_v) of the Native & Hy-HPMS* was estimated by determining their intrinsic viscosity values using capillary viscometry. A series of solutions were prepared by dilution of the respective *HPMS* solutions ensuring the concentrations lie within the *critical concentrations C* (denoted as 1/[η])*. Measurements of the capillary flow times of polymer solutions were performed using the type I Ubbelohde viscometer. Each measurement was performed at 20°C ± 0.1 under temperature-controlled water bath. To determine the M_v from the obtained flow rate values, Mark–Houwink equation was used as follows:

$$[\eta] = KM_v^{\alpha} \tag{2}$$

where, α and K are the Mark–Houwink equation constants specific to the polymer and solvent system used at given temperature conditions. For HPMS the pre-determined parameters in association with water are $\alpha = 0.88$, K = 3.39×10^{-4} (dL/g g/mol) $^{-\alpha}$.

The intrinsic viscosity [η] (dL/g) was determined using the common intercept of the individual Huggins and Kraemer extrapolations to zero polymer concentration via linear regression Equation (3):

$$[\eta] = \left(\frac{\eta_{sp}}{c}\right)_{C=0} = ln\left(\frac{\eta_{rel}}{c}\right)_{C=0} \tag{3}$$

© STM Journals 2026. All Rights Reserved

Here, η_{sp} *and* η_{rel} represent the specific and relative viscosities, respectively, while C denotes the polymer concentration (g/dL). Utilizing both plots allows for a more accurate determination of $[\eta]$. The obtained M_v values are compiled in Table 1.

Size Exclusion Chromatography (SEC)

SEC analysis was performed on the *Native and Hy-HPMS* polymer samples to obtain both Weight average molecular weight *(M_w)* and number average molecular weight (M_n) along with polydispersity value ($PD = M_w/ M_n$) of the polymers. SEC analysis was carried out on *(Infinity II*, *1260 GPC/SEC) Agilent Instruments, USA.*

The entire experiment was accomplished using buffer solution of *pH = 7* (which is a mixture of *0.2 N* $NaNO_3$ *and 0.01M* NaH_2PO_4). All the samples were prepared by solubilizing *20 mg* of the polymer *in 40 ml* of buffer and rested for *5h* for complete dissolution. To prevent the contamination of the undissolved macroparticles, prepared solutions were passed through a *0.5µm PVDF filter* before transferring into the sample vials. *Pl-aqua gel-OH column* was attached in series with Guard column, *8µm* diameter employed for the size exclusion at *30°C* temperature and *0.5 ml/min* flow rate. The eluents from the column are guided to the multi detector system equipped with RI, Viscosity and LS detectors. Before analysis, the SEC system was calibrated using the Pullulan Polysaccharide standards over the molecular weights range *800–0.18 kg/mole*. The Mw, Mn and PD data calculated by analyzing the SEC data using *Agilent Cirrus GPC software*.

CHARACTERIZATION OF NATIVE & HY-HPMS-PARACETAMOL SPIRULINA MICRO PELLETS

Scanning Electron Microscopy Imaging

To examine the Surface-morphology and the layers formation in the *Hy-HPMS* Paracetamol based microspheres SEM analysis was carried out using *JEOL JSM-5800 SEM (Japan)* operated at 15 kV. For imaging, the *Hy*-HPMS and paracetamol coated microspheres were deposited onto the metal stubs using double sided carbon tape, for cross sectional imaging microspheres were split into two half using sharp razor blade and carefully mounted on the stubs facing the cut interface upside. The stubs bearing microspheres then sputter coated with gold–palladium plasma coater to avoid charging in high vacuum mode. The imaging was done at *15 kV*, under high vacuum, with backscattering electrons imaging to locate coating regions, followed by secondary electrons imaging for surface morphology.

Dissolution Study

The in vitro dissolution study of the *Hy-HPMS*-coated micro-pellet-filled capsules was conducted using a USP Type I (basket) apparatus on an Electro lab Inspire 8000 automated system. The rotation speed was maintained at 50 rpm in 900 mL of simulated gastric fluid (SGF, pH 1.2), with the temperature held constant at 37 ± 1°C. Samples were automatically withdrawn at predetermined intervals of 0, 4, 8, 12, 16, 20, 24, 28, 32 minutes, with 10 mL aliquots collected into cuvettes. From each aliquot, 2 mL was transferred into a 100 mL volumetric flask and diluted to volume with deionized water. The diluted samples were further analyzed for drug content using UV spectrophotometry (Shimadzu UV–Vis, Japan) at 249 nm to quantify the amount of drug released from the micro-pellets.

Disintegration Study

The *in vitro* disintegration study was carried out on six capsules from each formulation – *Native* and *Hy-HPMS*-coated micro pallet-filled capsules – using a *Lab-India Disintegration Tester (DT 2000S, India)* with deionized water as the disintegration medium. The water bath temperature was maintained at *37 ± 1°C*. Disintegration of the coated microspheres was defined as the point at which no sphere residue remained in the bowl and no visibly firm core was present on the screen. Disks were used in accordance with USP requirements.

To evaluate the effect of temperature, capsules filled with microspheres were preconditioned at *37 ± 1°C*, and all four sets were analyzed. The preheating duration ranged from *30 to 60* minutes to satisfy

© STM Journals 2026. All Rights Reserved

the requirements of the full factorial design under controlled humidity. For each formulation, four sets of capsules were preheated; one set was tested immediately after preheating, while the other was allowed to cool to room temperature for *30 minutes* prior to testing. Disintegration times for each formulation were recorded at one-minute intervals, and the procedure was performed following the *USP method*.

RESULTS AND DISCUSSION

Molecular Weight Analysis, Hydrogen Bonding Interactions of HPMS

As illustrated in Schematic 1. the stepwise mechanism of acid hydrolysis involves the treatment of high molecular weight HPMS polymer chains with hydrochloric acid at varying concentrations to obtain a target molecular weight suitable for spray coating on glucose microspheres. The hydrogen ions (H^+) from the acid selectively attack the α-1,4-glycosidic amylose bonds and also some part of α-1,6-glycosidic amylopectin bonds connecting glucose units in the starch backbone. Protonation of the glycosidic oxygen increases the bond's electrophilicity, rendering it more prone to cleavage and resulting in progressive chain scission. This degradation process effectively reduces the molecular weight of the polymer. The resulting molecular weight in the hydrolyzed HPMS were subsequently analyzed and validated using viscometry and size exclusion chromatographic method (Figure 1).

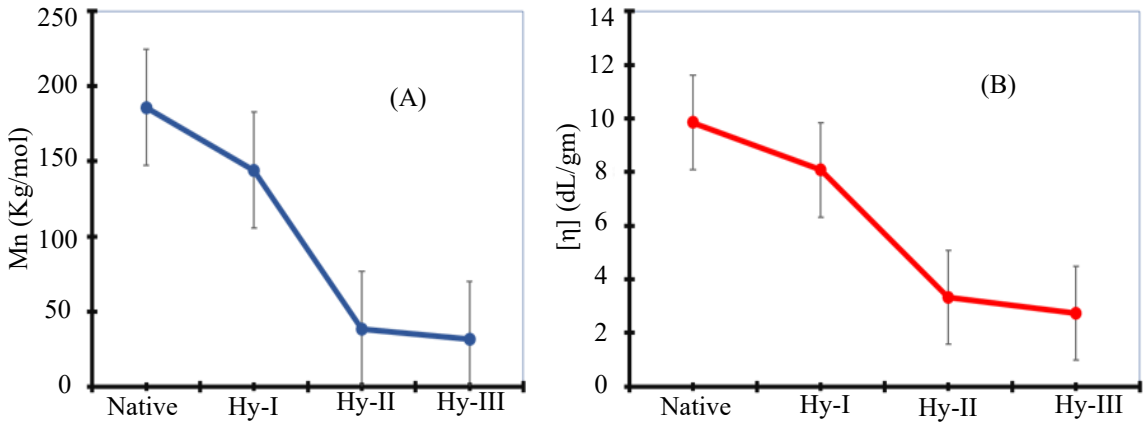
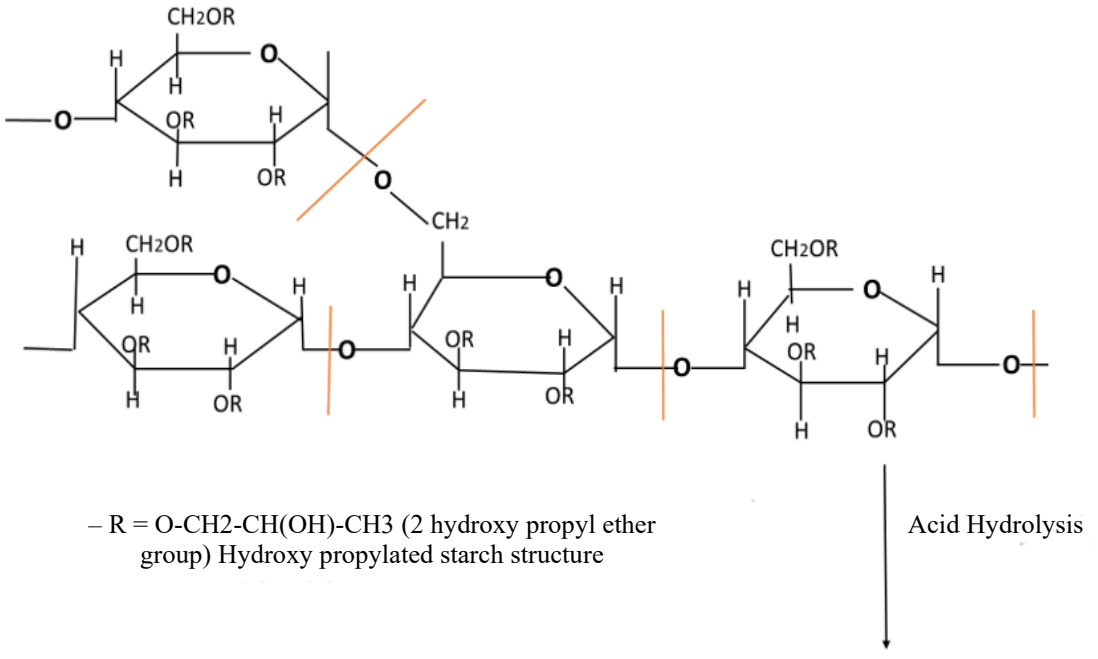
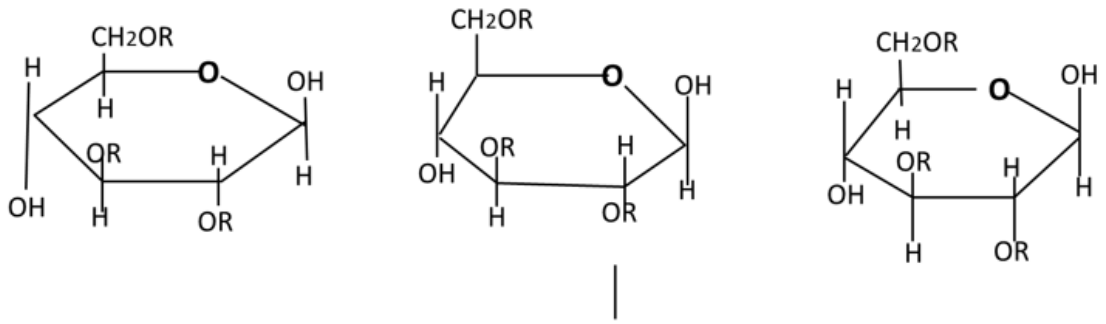


Figure 1. Capillary viscometry, GPC data of the unhydrolyzed and hydrolyzed HPMS samples.



© STM Journals 2026. All Rights Reserved



– R = O-CH_2-CH(OH)-CH_3 (2 hydroxy propyl ether group) Glucose, Dextrin & oligosaccharides with hydroxy propyl structure

Schematic 1. Step wise mechanism of HPMS hydrolytic degradation.

Molecular Weight Analysis

The degradation behavior of *hydroxy propylated starch (HPMS)* polymer upon acid hydrolysis was investigated by analysing changes in molecular weight before and after treatment. Capillary viscometry, a rapid and convenient technique, was employed as the primary method to evaluate the *number-average molecular weight (Mn) and intrinsic viscosity ([η])* of the polymer. Figure 1(a–b) illustrates the variation *of [η] and Mn* as a function of sample composition, providing an initial insight into the extent of hydrolytic degradation.

To enhance the accuracy and provide a comparative perspective, *size-exclusion chromatography (SEC) coupled with tri detector system (RI-VISCO-LS)* was utilized. Despite the widespread use of *HPMS*, there have been no previous reports focusing on the molecular weight analysis of the *single-grade Lycoat 780 HPMS*, making this investigation particularly relevant.

A summary of the *viscometrical ([η], Mv) and SEC (Mn, Mw, and polydispersity index, PD)* data is presented in Table 1. From the results, capillary viscometry measurements revealed a significant decrease in intrinsic viscosity from *9.84 to 2.73 dL/g* as the extent of acid hydrolysis increased. By applying the Mark–Houwink equation, Mn values were calculated for each degraded polymer solution, showing a decline from *186.02 kg/mol* in the pristine sample to a limiting value of *31.339 kg/mol* after three hours of hydrolysis under controlled conditions.

Table 1. Capillary viscometry, GPC data of the unhydrolyzed and hydrolyzed HPMS samples.

	Capillary viscometry		**GPC**		
	[η]	M_v	M_w	M_n	
Sample code	**(dL/g)**	**(kg/mol)**	**(kg/mol)**	**(kg/mol)**	**PD**
Native-HPMS	9.8475	397.738	556.82	186.02	2.993
Hy-HPMS-I	8.0819	269.554	354.576	144.212	2.450
Hy-HPMS-II	3.3202	59.524	68.833	38.345	1.749
Hy-HPMS-III	2.7314	41.368	45.354	31.339	1.447

The SEC measurements of Mn and Mw corroborated the viscometric findings, despite differences in sample preparation and analytical principles between the two techniques. This consistency underscores the reliability of the observed molecular weight reduction. Importantly, all molecular weight measurements were based on a minimum of two independently prepared and hydrolyzed solutions derived from the same polymer batch, ensuring reproducibility and accuracy.

These results collectively confirm the pronounced degradation of *HPMS* molecular weight during acid-mediated hydrolysis and establish a baseline for future studies involving this specific polymer

© STM Journals 2026. All Rights Reserved

grade. Polydispersity *(PD)* values obtained from SEC measurements revealed that the pristine *HPMS* exhibited a molecular weight polydispersity of 2.993, indicating a relatively different particles polymer distribution. Interestingly, a slight improvement in polydispersity was observed in the case of *hy*-HPMS *III*, with a reduced PD value of 1.447, suggesting the formation of more uniform, unimolecular-weight polymer segments because of mild hydrolytic degradation.

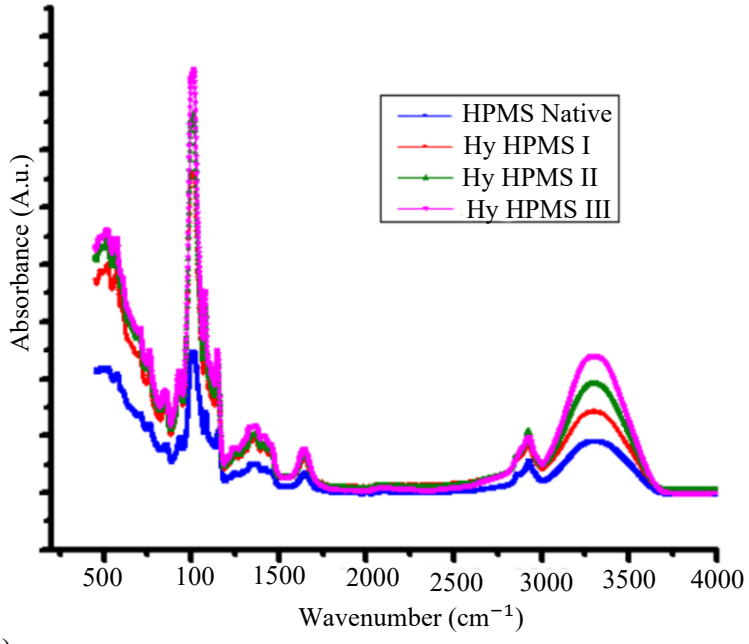
However, exposure to higher acid concentrations (as in *Hy*-HPMS *II* and *Hy*-HPMS III) led to a significant decrease in polydispersity. This indicates the generation of increasingly homogeneous polymer segments with a broader range of molecular weight distributions. The observed changes in molecular weight characteristics – PD, [η], Mv, Mw, and Mn – correlate well with variations in thermal characteristics, mechanical strength, coating performance, and dissolution behavior, as discussed in subsequent sections.

FTIR-ATR Spectra Analysis

The Native & degraded HPMS solutions were cast into thermoplastic films (Figure 1) at room temperature under a controlled relative humidity of 55%. The resulting films appears identically clear and transparent, were analyzed using FTIR in ATR mode shown in Figure 2(a–c).

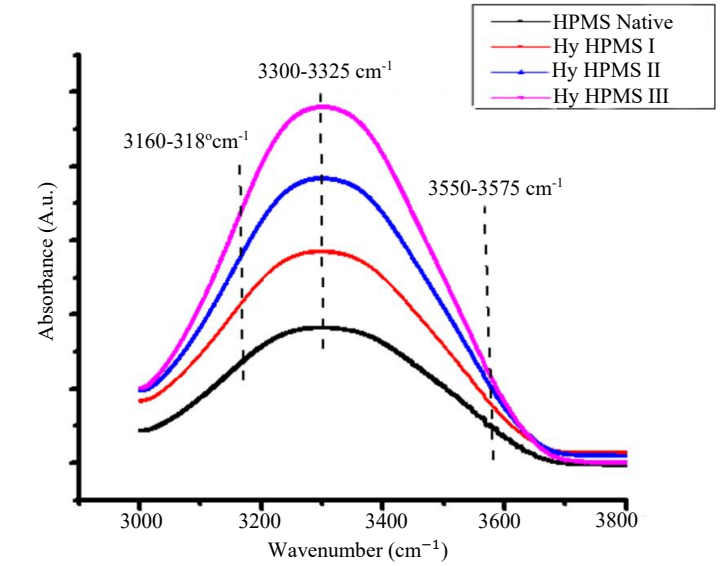
Specifically, this section discusses the hydrogen bonding interactions in hydrolytically degraded HPMS polymers. As shown in Figure 2(a), the overlaid FTIR spectra of HPMS display characteristic absorption bands at 3300–3325 cm^{-1} (O–H stretching vibration often broaded by hydrogen bonding),3550–3375 cm^{-1} rage typically indicates hydrogen bonded O–H (hydroxyl stretching vibration which is common in alcohol, 2920 cm^{-1} (C–H stretching), and 1050–1000 cm^{-1} (C–O–C stretching) for primary alcohol, confirming the presence of hydroxy, methyl, and ether functional groups. The region corresponding to –O–H stretching relevant for interpreting hydrogen bonding interactions in HPMS.

In Figure 2(b), a partial peak centered at 1620 cm^{-1} is observed, typically attributed to O–H bending (H–O–H scissoring) of adsorbed water molecules. As previously reported, this peak does not arise from the intrinsic polymer backbone (e.g., C=O or C=C) but rather indicates the presence of physically adsorbed or bound water. Notably, the intensity of this peak increases progressively with the degree of hydrolytic degradation, suggesting enhanced water uptake due to increased availability of hydrophilic sites (Figure 2(a)).

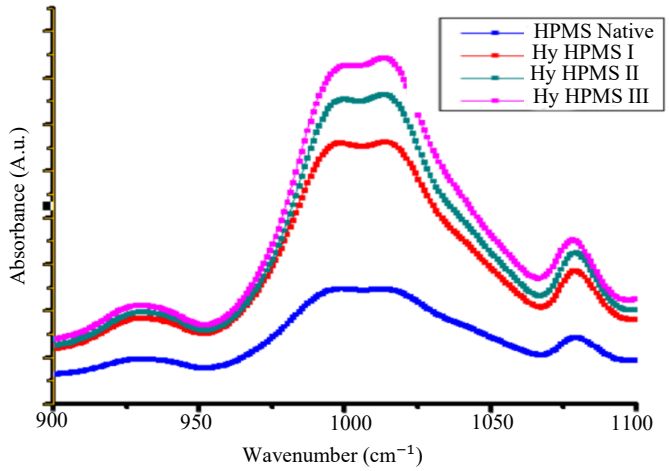


(a)

© STM Journals 2026. All Rights Reserved



(b)



(c)

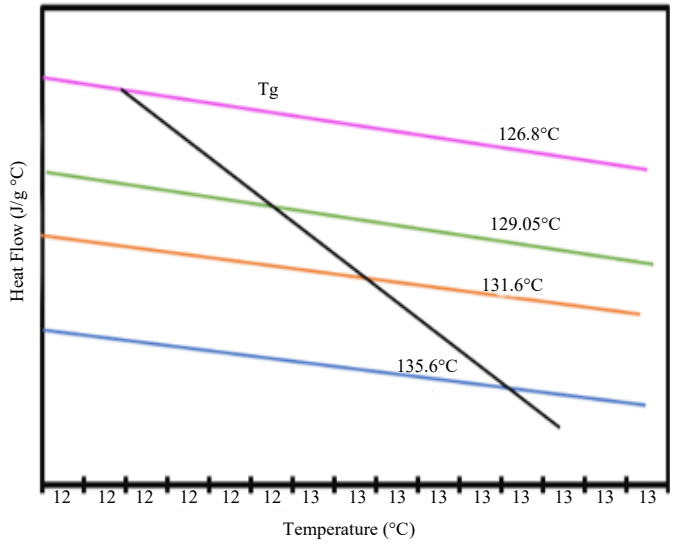
Figure 2. FTIR-ATR spectra of *Hy*-HPMS: (a) overlayed full spectra of Native and hydrolyzed HPMS, (b) Partial spectra attributed to O–H bending (H–O–H scissoring) of adsorbed water molecules, and (c) partial spectra of hydrogen-bonded –OH groups.

Similarly, Figure 2(c) presents the O–H stretching region associated with intermolecular hydrogen bonding within the polymer matrix. The primary peak, located between *3550–3575 cm⁻¹*, corresponds to hydrogen-bonded –OH groups, while a prominent shoulder peak in the *3300–3325 cm⁻¹* range is attributed to free –OH groups. The increase in intensity of both peaks with advancing hydrolysis indicates a higher concentration of –OH groups and consequently stronger or more extensive hydrogen bonding within the polymer matrix. Overall, FTIR analysis revealed that the characteristic peaks of undegraded and degraded HPMS remained largely similar. The functional group absorptions of native HPMS exhibited no significant shifts or alterations following hydrolysis, and no additional peaks were detected. This indicates that no new functional groups were formed and that the primary pyranose ring structure of HPMS was preserved. Notably, a decrease in the intensity of glycosidic bond absorption at 1020 cm^{-1} was observed, suggesting that acid hydrolysis induced cleavage of intermolecular glycosidic linkages, thereby reducing their abundance. These observations are consistent with earlier reports demonstrating that cellulosic materials generate degradation products upon degradation [30] and confirm that HPMS undergoes disruption of intermolecular glycosidic bonds during hydrolytic degradation.

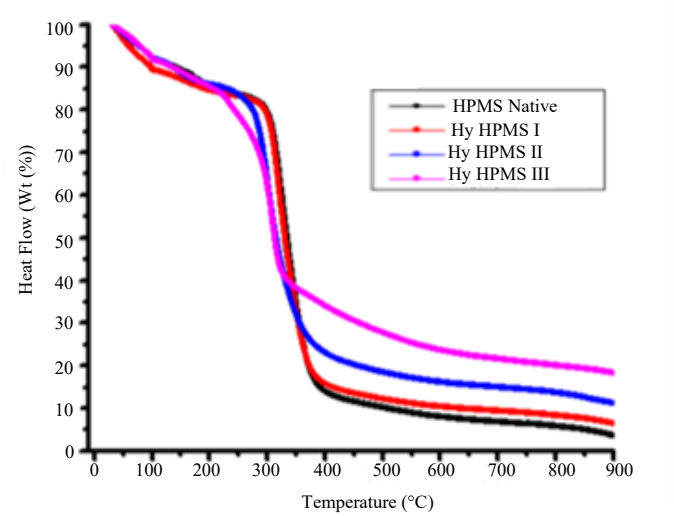
© STM Journals 2026. All Rights Reserved

Thermal Characteristics of the *Hy*-HPMS Films

The thermal behavior of native and hydrolytically degraded HPMS samples was examined using DSC and TGA to evaluate their thermal transitions in relation to structural integrity. Figure 3(a) presents the stacked plots of heat flow versus temperature for all samples. The native sample exhibited a glass transition temperature of 135.6 ± 3°C. Following hydrolytic degradation, this value decreased significantly to 126.8 ± 2°C, indicating decreased chain entanglement and enhanced segmental mobility. This observation aligns well with molecular weight data obtained from GPC and viscometry. Comparative TGA thermograms of native and degraded HPMS (Figure 3(b)) reveal that hydrolytic degradation has only a minimal effect on the overall thermal stability of the polymer. All samples display a single degradation event occurring between 390–450°C (Figure 2) with only a slight shift attributable to degradation. A key finding is that chain scission generates additional terminal hydroxyl groups, increasing the hydrophilic nature of the polymer. This is reflected in the observed weight loss below 100°C, corresponding to moisture evaporation. The moisture loss follows the order: Native < *Hy*-HPMS I < *Hy*-HPMS *II* < *Hy*-HPMS III, which is consistent with the LOD values (Table 2). Overall, these results demonstrate that hydrolytic degradation markedly influences the glass transition temperature, moisture retention, and degradation behavior of HPMS samples, highlighting the role of acid-mediated hydrolysis in altering their thermal and structural properties



(a)



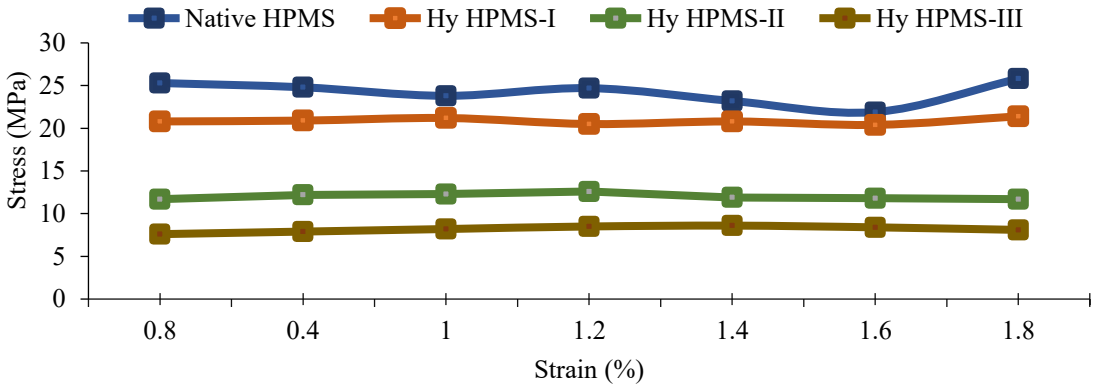
(b)

Figure 3. Thermal properties of the native and *Hy*-HPMS samples: (a) DSC measurements, (b) TGA measurements.

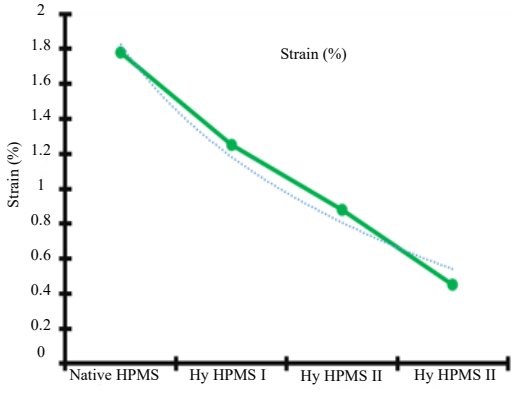
© STM Journals 2026. All Rights Reserved

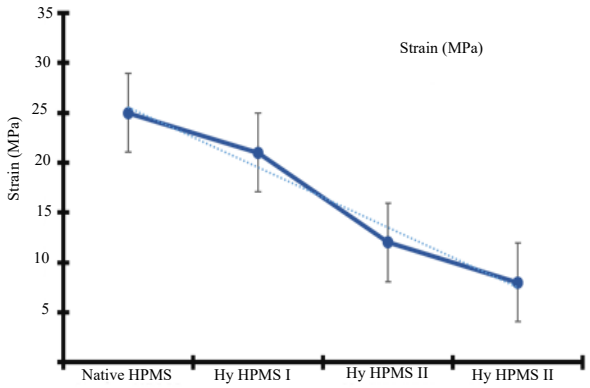
Tensile Properties of Hy-HPMS

The mechanical properties of the untreated and hydrolyzed HPMS were presented in Figure 4; (a) the compiled stress vs strain plots, (b) Linear fitting plot of the stress vs composition, and (c) linear fitting plot of strain (%) vs composition. Their mechanical performance data is summarized in Table 2. The film made from native HPMS (*Lycoat RS 780*) grade showed remarkable tensile strength under control conditions at 65% relative humidity and 23°C. The tensile properties of the HPMS can be significantly affected by hydrolytic degradation, particularly under acidic conditions and elevated temperatures. This effect is reflected on the stress vs strain profiles of the hydrolyzed films, the break stress and the elongation at break for the native samples found to be 24.9 ± 2 MPa and 1.9 ± 0.8%, respectively. Which has dropped significantly for the hydrolyzed samples there is clear monotonic drop in the stress, toughness and young's modulus (Figure 4(a–c)) upon varying the degree of hydrolysis. It was visibly noticed; higher the percentage of the HCl added lower the tensile strength of the films.



(a)





(b) (c)

Figure 4. Conventional uniaxial tensile test. The comparative plot of the mechanical behavior of the Hy-HPMS films evidenced the loss in the mechanical properties resulting from hydrolysis. (a) The compiled stress vs strain plots, (b) linear fitting plot of strain (%) vs composition, and (c) Linear fitting plot of the stress vs composition.

This phenomenon can be explained by the fact that, upon hydrolysis, the glycosidic bonds in the starch amylose & amylopectin backbone of HPMS are cleaved, leading to a reduction in the polymer's molecular weight. The molecular chain scission disrupts the continuity of the polymer matrix, resulting in shorter chain lengths that are less capable of entanglement and intermolecular interaction.

© STM Journals 2026. All Rights Reserved

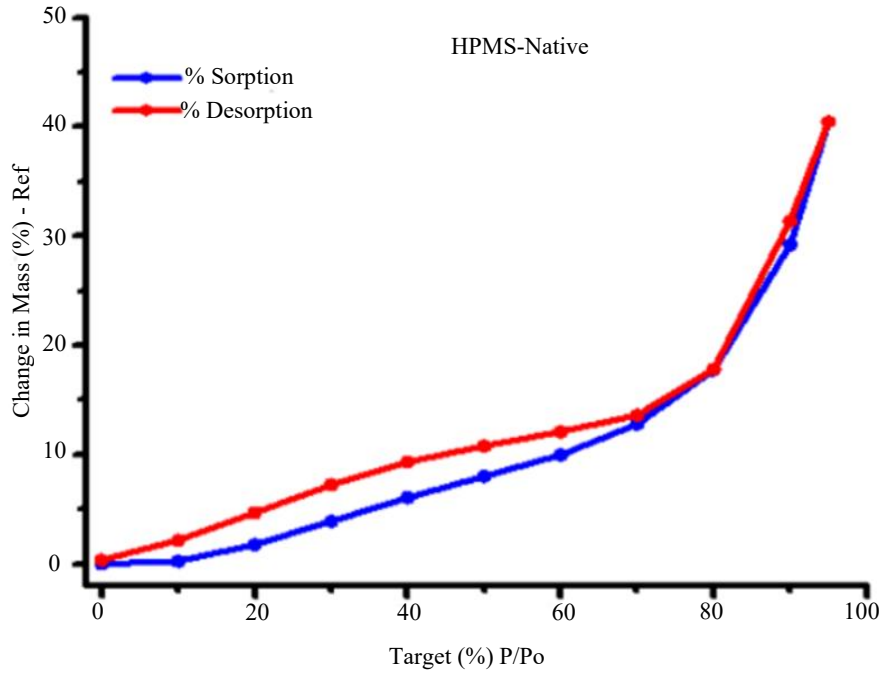
In contrast, the break strain of the samples also exhibits significant variation with the extent of hydrolysis. This phenomenon can be attributed to the moisture retention behavior of the polymer, as supported by the Loss on Drying (LOD) measurements (Table 2). Although hydrolysis leads to a decrease in molecular weight and compromises the cohesive strength of the film due to chain scission, the increased moisture content appears to preserve the flexibility of the polymer matrix. Consequently, the tensile elongation properties remain relatively unaffected. These observations align well with the molecular weight degradation analysis discussed earlier, reinforcing the correlation between hydrolytic effects and the mechanical performance of HPMS films.

Table 2. Tensile properties. tensile strength (MPa), strain at break (%), young's modulus (E), and toughness (area under the curve, MPa) of films based on degree of hydrolysis of the HPMS films.

Sample code	Stress (MPa)	Strain (%)	LOD (W%)
Native	24.9 ± 1.9	1.9 ± 0.9	10.7 ± 0.04
Hy-HPMS-I	20.8 ± 1.5	1.25 ± 0.5	13.0 ± 0.03
Hy-HPMS-II	12.9 ± 1.3	0.88 ± 0.3	15.1 ± 0.03
Hy-HPMS III	8.4 ± 0.8	0.5 ± 0.2	18.2 ± 0.04

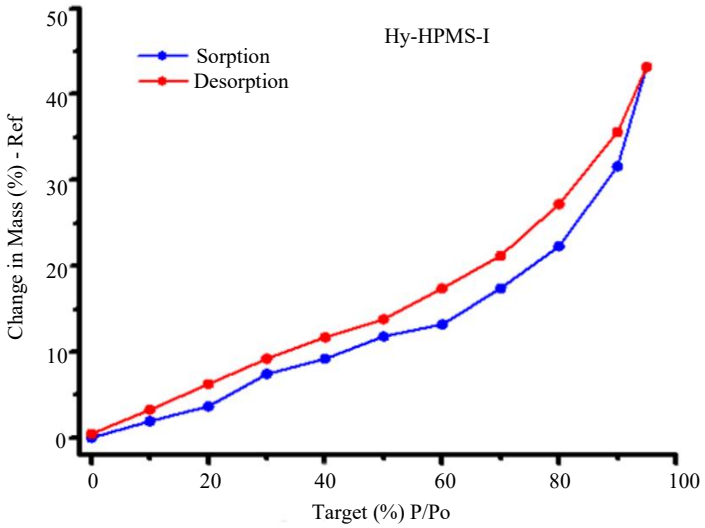
Vapor Sorption Behavior of Native & *Hy*-HPMS

Dynamic vapor sorption (DVS) provides gravimetric data for samples under precisely controlled environmental conditions such as relative humidity (RH) and temperature. This technique has been extensively applied to amorphous systems, including the quantification of amorphous content within crystalline materials, the assessment of polymer stability, and the investigation of molecular interactions between drug substances and polymers in solid dispersions [31]. In order to investigate the variation in HPMS affinity towards water before and after hydrolytic treatment DVS was employed. A typical water sorption and desorption isotherms, which reflects the interaction between water and the material, shows the mass change of the mixture caused by water uptake at a specific temperature and pressure [31–33]. The complete cycle of the moisture sorption and desorption isotherms of the native and hydrolytically degraded HPMS samples at 25°C are illustrated in Figure 5(a–d).

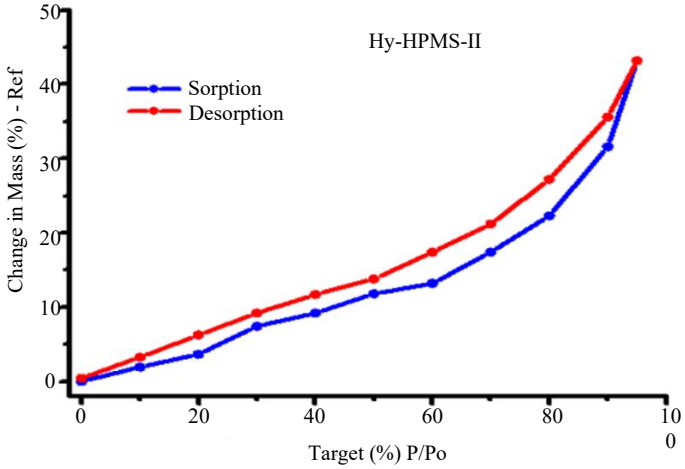


(a)

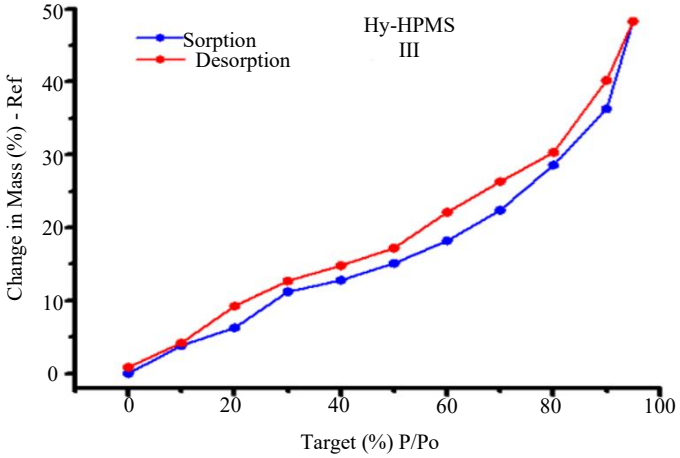
© STM Journals 2026. All Rights Reserved



(b)



(c)



(d)

Figure 5. The complete cycle of moisture sorption and desorption isotherms of the Native and hydrolytically degraded HPMS samples.

© STM Journals 2026. All Rights Reserved

The percentage weight gain at the end of the test is reported in Table 1 for all tested HPMS films. The change in masses of the Native HPMS, *Hy*-HPMS *I*, *Hy*-HPMS *II and Hy*-HPMS III were 40.7%, 43.2%, 46.8% and 48.3 at 95% RH, respectively, where the RH of Native sample is in great agreement with values reported by manufacturers [34]. The rise in the water vapor affinity of the hydrolytically degraded HPMS is reflected clearly in the FTIR spectrum as discussed earlier in Figure 2. The change in mass percentage up to 60°C is found to be almost similar in all the cases (Table 1), which indicates even after degradation the polymer water sorption properties like great extent which helps to use these partially degraded sample to wide range of applications. Another important observation is the gap between sorption and desorption cycle has increased in the fashion Native < *Hy*-HPMS I < *Hy*-HPMS II < *Hy*-HPMS *III*. The native sample has closer sorption and desorption isotherms compared to degraded samples, the increase in the gap indicates more water retention during sorption and relatively slower release rate during desorption shows increase in the hydroxyl functional groups as a result of cleavage of glycosidic linkages in the starch backbone of HPMS. These attributes are greatly corroborated by GPC-derived Mw reduction and FTIR/DSC evidence of chain scission and lowered T_g, provide a quantitative justification that acid hydrolysis fundamentally alters HPMS–water interactions."

Thermo-Reversible Gelling Properties of the *Hy*-HPMS

Hydroxypropyl starch (HPMS) undergoes phase separation from water when the temperature of its aqueous solution is raised beyond a certain threshold, primarily due to molecular chain aggregation [35]. This aggregation is driven by hydrophobic interactions between methoxy and hydroxypropyl substituents on the HPMS backbone [36]. Several techniques, including calorimetry, rheometry, and light scattering, have been employed to elucidate the thermal gelation behavior of HPMS solutions [36, 37]. Jin et al. (2013) successfully demonstrated the hysteresis phenomenon in the gelation behavior of aqueous HPMS during heating and cooling cycles [**Error! Reference source not found.**].

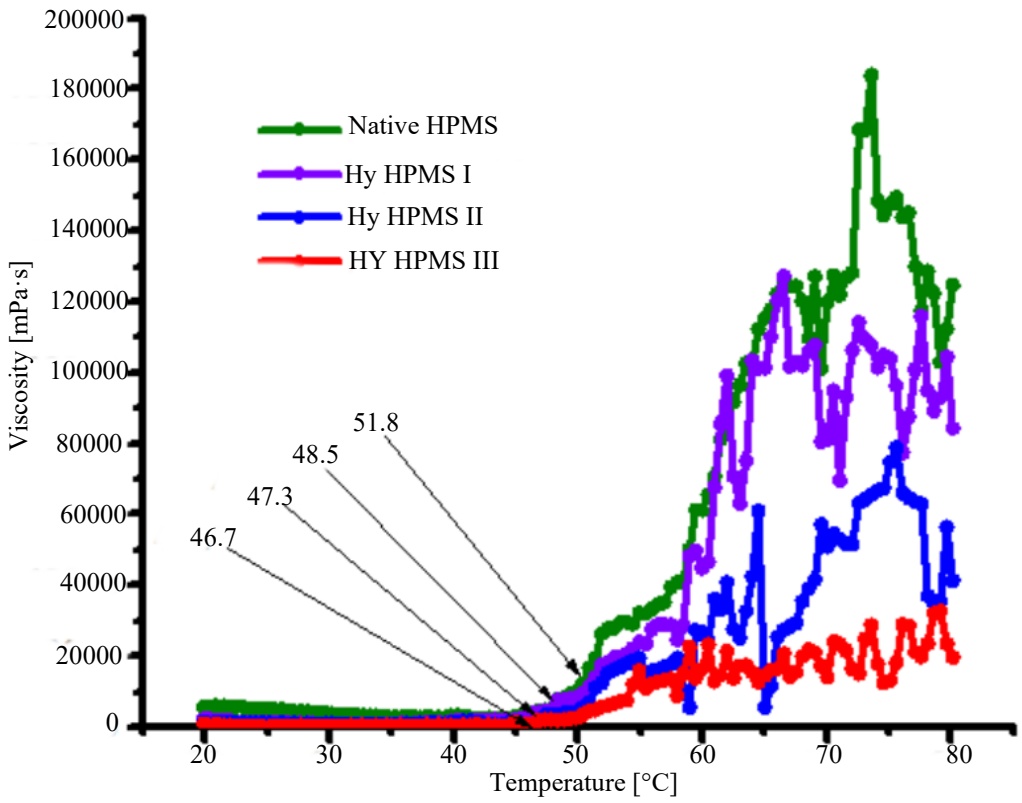
In the present study, a similar rheometric approach – the steady-shear temperature sweep – was adopted to investigate the effect of hydrolytic degradation on HPMS gelling properties. Figure 6(a) illustrates the influence of temperature on the shear viscosity of native and hydrolytically degraded HPMS samples, measured at a heating rate of 0.5°C min^{-1} for 42% (w/v) aqueous solutions. No significant change in shear viscosity was observed up to 42°C. Native HPMS began to gel at 51.8 ± 0.5°C, reaching maximum gelation at 72 ± 0.5°C with a viscosity of 1.49×10^5 mPa·s, consistent with previously reported literature values [39]. Hydrolytic degradation led to a pronounced shift in gelation onset, with values of 48.5 ± 0.5°C, 47.3 ± 0.5°C, and 46.7 ± 0.5°C for *Hy*-HPMS I, *Hy*-HPMS *II*, and *Hy*-HPMS *III*, respectively – significantly lower than the native sample. This trend was also reflected in the kinematic viscosity results (Figure 6(b)), obtained under constant temperature and shear rate. Notably, the maximum gelling-point viscosities of *Hy*-HPMS *I* and *Hy*-HPMS *II* were comparable to that of the native material, suggesting that fully gelled samples possess similar gel network strengths despite the lowered gelation temperatures. In contrast, *Hy*-HPMS III exhibited a substantial reduction in both maximum gelling temperature and peak viscosity, likely attributable to a broader molecular weight distribution and higher polydispersity. These rheological observations align closely with results from complementary analyses, providing strong cross-validation for the findings of this study.

Coating Properties

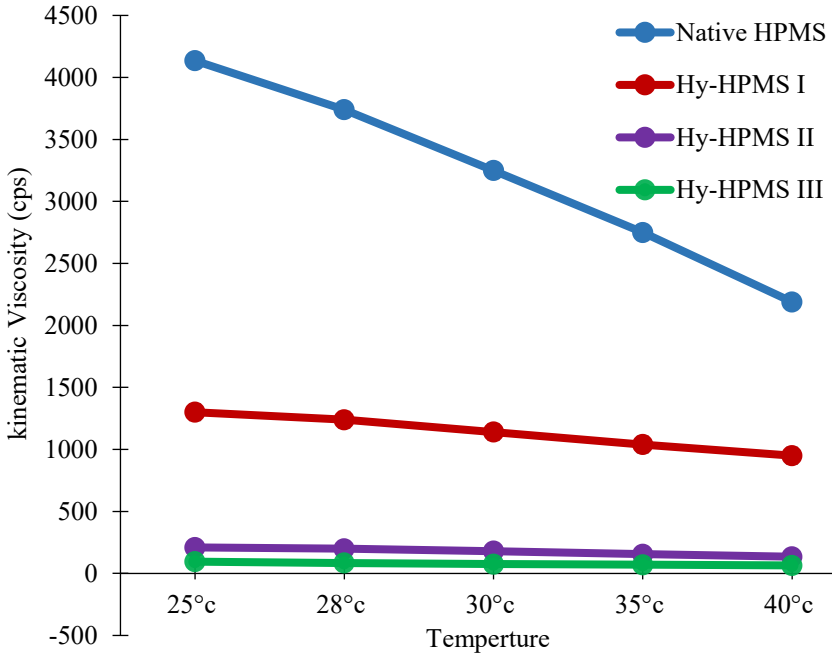
Previous studies have demonstrated that the viscosity grade of HPMS polymers plays a crucial role in modulating the drug release behavior of coated microspheres [40].

In the present study, the synthesis of three-layered HPMS–paracetamol coated microspheres was carried out using a spray coater (Schematic 2). The coating process employed ethanol–HPMS solutions (20–25% w/v) at varying polymer concentrations and spray flow rates. The native HPMS spray-dried microspheres served as control and prepared following three sequential coating steps – (i) base HPMS layer, (ii) paracetamol drug layer, and (iii) a final seal coat – the material yield reached approximately 99.3% (Table 3). Field-emission scanning electron microscopy (FE-SEM) imaging (Figure 7) clearly identified the three distinct layers in cross-section: the base coat tightly adhered to the sugar core, the intermediate paracetamol layer, and the final seal coat distinctively appear separate.

© STM Journals 2026. All Rights Reserved



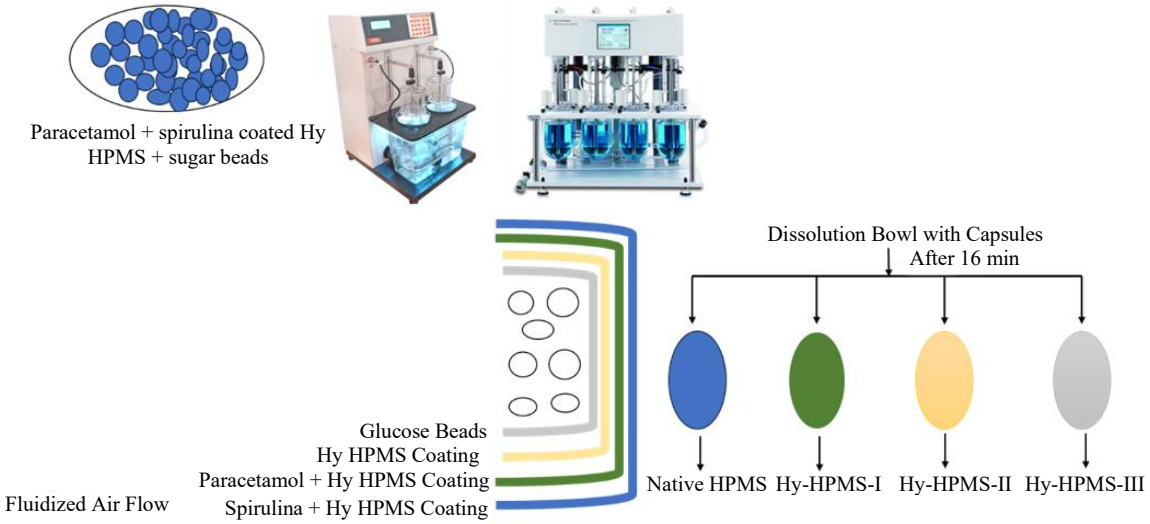
(a)



(b)

Figure 6. (a) The steady-shear viscosity plots of the aqueous HPMS solutions as a function of temperature measured in heating mode. (b) Kinematic Viscosity value of the HPMS solutions at 25°C, 28°C, 30°C 35°C, 40°C.

© STM Journals 2026. All Rights Reserved



Schematic 2. Synthesis and dissolution process of three-layered HPMS-paracetamol coated microspheres using Wurster coater.

Table 3. Loss on drying (LOD), viscosity and yield (%) of coating solution viscosity and coating yield %.

HPMS Ly coat RS780	**LOD**	**Viscosity**	**Yield**
Material	*(%)*	*cps*	*(%)*
Pristine	13.8	125	88.8
Hy-HPMS I	15.4	85	93.3
Hy-HPMS II	18.8	69	98.4
Hy-HPMS III	19.3	32	99.9

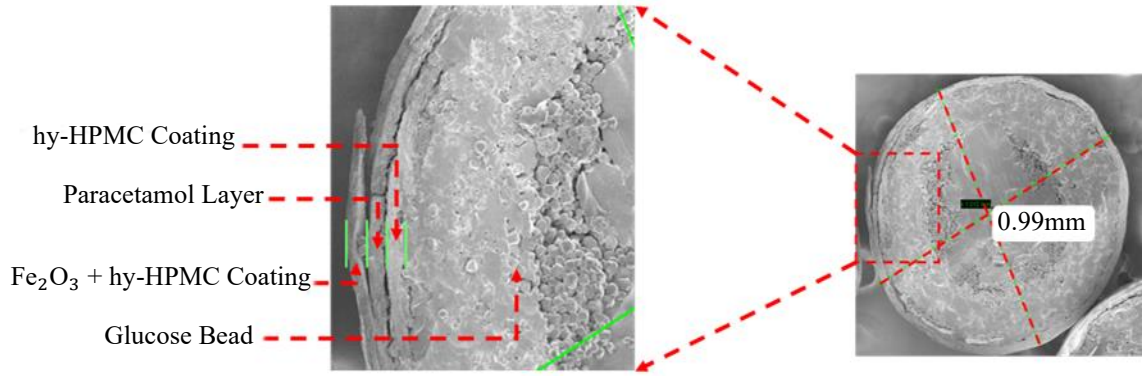


Figure 7. FE-SEM image of the coated microspheres incest enlarged image of the coated layers.

Notably, the seal coat surface exhibited non-uniformity, with visible microdroplet spots suggesting uneven HPMS distribution. This irregularity is attributed to the high viscosity (60 cps, Table 3) of the coating solution, which likely impaired atomization and reduced water retention capacity.

Hydrolytic degradation of the polymer markedly improved coating performance. Material yield increased to 88.8–99.9%, and surface uniformity was significantly enhanced across all degraded samples. Viscosity decreased from 125 cps to 32 cps for the hydrolytically degraded variants (Hy-HPMS I, Hy-HPMS II, and Hy-HPMS III), while loss on drying (LOD) values rose from 13.8% to 19.3%, indicating improved water-holding capacity during atomization (Table 3). This facilitated more uniform coating deposition, as confirmed by SEM analysis, which revealed the absence of clearly distinguishable layers – suggesting improved adhesion between coating strata and smoother surfaces.

© STM Journals 2026. All Rights Reserved

The enhanced adhesion characteristics of acid-mediated, hydrolytically degraded HPMS were further validated through dissolution studies, confirming their influence on drug release behavior. These findings underscore the importance of polymer viscosity and molecular modification in optimizing microsphere coating performance and drug release properties.

Dissolution Study

The goal of this study is to understand the influence of acid mediated hydrolysis on the drug releasing profiles of Paracetamol–HPMS coated microspheres. Figure 8 represents the compiled drug release (%) Vs time plot of the prepared capsules and the corresponding data presented in Table 4. The release profile of capsules containing native HPMS-coated paracetamol microspheres demonstrated a complete drug release (100%) within 30.0 ± 2.0 minutes (Table 4) in simulated gastric fluid (SGF, pH 1.2). The obtained release profile clearly indicates that paracetamol exhibited a pulsatile release behavior, suggestive of diffusion-controlled release through a gelled HPMS matrix – characteristic of a network formed by entangled high molecular weight polymer chains. In contrast, hydrolyzed HPMS (Hy-HPMS) samples showed significantly faster drug release, achieving complete (100%) release within 18 to 24 minutes.

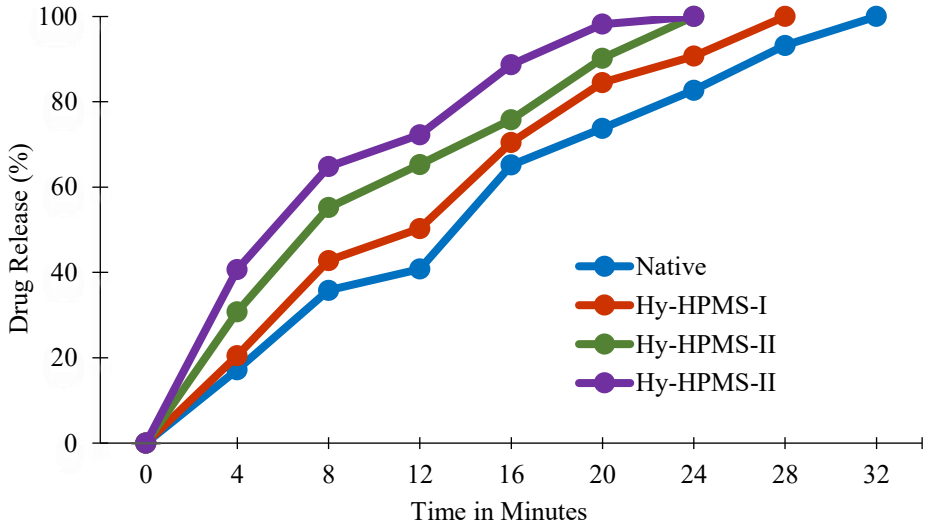


Figure 8. Effect of degree of hydrolysis on paracetamol release from *HPMS-coated paracetamol*.

The time required for 40% drug release followed the order: Hy-HPMS III < Hy-HPMS II < Hy-HPMS I, indicating that acid-mediated hydrolysis of HPMS plays a crucial role in modulating the drug release kinetics (Schematic 2). Highlighting an enhanced diffusional release profile corresponding to higher drug solubility.

Table 4. Drug release performance of the Native and hydrolyzed HPMS samples.

Time (min)	Native	Hy-HPMS-I	Hy-HPMS-II	Hy-HPMS-III
0	0	0	0	0
4	17.2	20.5	30.8	40.7
8	35.8	42.8	55.2	64.8
12	40.8	50.3	65.3	72.3
16	65.2	70.5	75.8	88.7
20	73.8	84.5	90.2	98.2
24	82.7	90.7	100	100
28	93.2	100	–	–
32	100	–	–	–

© STM Journals 2026. All Rights Reserved

These findings underscore that acid hydrolysis is an effective strategy to fine-tune the release characteristics of HPMS-coated paracetamol microspheres, and more broadly, it offers a promising approach to customize the drug release profiles in various pharmaceutical dosage forms.

Disintegration Study (Lowenthal, 1973; Pilpel et al., 1978; Gordon et al., 1993; Carter, 2002; Carter, 2002)

The disintegrant action of native and hydrolyzed HPMS is primarily driven by swelling, wicking, and particle deformation–recovery. Fluid uptake initiates wicking, followed by elastic recovery of compressed starch particles, which releases internal stresses and disrupts hydrogen-bond networks, enabling pellet-fill disintegration.

Disintegration efficiency increased with the degree of acid hydrolysis, following the order Hy-HPMS III < Hy-HPMS II < Hy-HPMS I < Native starch. Spirulina-coated pellets fully disintegrated in approximately 3 min (Hy-HPMS III), 4 min (Hy-HPMS II), 6 min (Hy-HPMS I), and 10 min (native starch).

Extra granular incorporation of HPMS provided faster disintegration than intragranular addition due to greater accessibility. Overall, the extent of acid hydrolysis is a key factor shaping HPMS particle properties and enhancing its disintegrant performance.

CONCLUSION

In summary, we demonstrated that a simple acid-mediated hydrolysis method can be employed to produce HPMS (*Lycoat RS 780*) polymer solutions with tuneable molecular weights and narrow polydispersity, depending on the concentration of acid used. To the best of our knowledge, this is the first report to describe HCl-mediated hydrolysis of HPMS and to characterize the physicochemical properties of films prepared from hydrolytically degraded polymers. The resulting films were systematically evaluated for mechanical strength, glass transition temperature (T_g), moisture retention, and viscosity, all of which exhibited clear trends correlating with the degree of hydrolysis. FTIR–ATR analysis provided qualitative evidence of increased –OH functionalities because of chain scission.

Furthermore, paracetamol-loaded hydrolyzed HPMS microspheres were successfully prepared using a spray-drying coater. The extent of hydrolysis was shown to significantly influence drug release from spirulina based HPMS–paracetamol–coated sugar microspheres. Dissolution studies revealed a clear trend in release times, following the order: *Hy*-HPMS III < *Hy*-HPMS II < *Hy*-HPMS I < Native HPMS, thereby confirming that acid-mediated hydrolysis of HPMS plays a crucial role in modulating release kinetics.

Overall, these findings highlight acid hydrolysis as a practical and effective strategy for fine-tuning the release characteristics of HPMS-coated paracetamol microspheres. More broadly, this approach offers a promising pathway for customizing drug release profiles across diverse pharmaceutical & Nutraceutical dosage forms.

REFERENCES

1. Bourtoom T, et al. Edible films and coatings: Characteristics and properties. Int Food Res J. 2008;15(3):237–248.
2. Embuscado ME, Huber KC, et al. Edible films and coatings for food applications. New York (NY): Springer; 2009. p. 169–208.
3. Von Schantz L, Schagerof H, Nordberg Karlsson E, Ohlin M, et al. Characterization of the substitution pattern of cellulose derivatives using carbohydrate-binding modules. BMC Biotechnol. 2014;14(1):113–119.
4. El Ghzaoui A, Trompette JL, Cassanas G, Bardet L, Fabregue E, et al. Comparative rheological behavior of some cellulosic ether derivatives. Langmuir. 2001;17(5):1453–1456.

© STM Journals 2026. All Rights Reserved

5. Goodwin DJ, Picout DR, Ross-Murphy SB, Holland SJ, Martini LG, Lawrence MJ, et al. Ultrasonic degradation for molecular weight reduction of pharmaceutical cellulose ethers. Carbohydr Polym. 2011;83(2):843–851.
6. Guo JH, Skinner GW, Harcum WW, Barnum PE, et al. Pharmaceutical applications of naturally occurring water-soluble polymers. Pharm Sci Technol Today. 1998;1(6):254–261.
7. Li J, Mei X, et al. Applications of cellulose and cellulose derivatives in immediate release solid dosage. In: Marchessault RH, Ravenelle F, Zhu XX, editors. Polysaccharides for drug delivery and pharmaceutical applications. ACS Symposium Series. Vol. 934. Washington (DC): Oxford University Press; 2006. p. 19–55.
8. Pfefferkorn P, Beister J, Hild A, Thielking H, Kulicke WM, et al. Determination of the molar mass and the radius of gyration, together with their distributions for methylhydroxyethylcelluloses. Cellulose. 2003;10(1):27–36.
9. Duro R, Alvarez C, Martinez-Pacheco R, Gomez-Amoza JL, Concheiro A, Souto C, et al. The adsorption of cellulose ethers in aqueous suspensions of pyrantel pamoate: Effects on zeta potential and stability. Eur J Pharm Biopharm. 1998;45(2):181–188.
10. Parker MD, York P, Rowe RC, et al. Binder-substrate interactions in wet granulation. 2: The effect of binder molecular weight. Int J Pharm. 1991;72(3):243–249.
11. Rowe RC, et al. The molecular weight and molecular weight distribution of hydroxypropyl methylcellulose used in the film coating of tablets. J Pharm Pharmacol. 1980;32(1):116–119.
12. Dahl TC, Calderwood T, Bormeth A, Trimble K, Piepmeier E, et al. Influence of physico-chemical properties of hydroxypropyl methylcellulose on naproxen release from sustained release matrix tablets. J Control Release. 1990;14(1):1–10.
13. Lusvardi KM, Harcum WW, Skinner GW, Durig T, et al. Fundamentals of hydroxypropyl cellulose binders in wet granulation. AAPS J. 2003;5:1744.
14. Müller RH, Keck CM, et al. Challenges and solutions for the delivery of biotech drugs—A review of drug nanocrystal technology and lipid nanoparticles. J Biotechnol. 2004;113(1–3):151–170.
15. Keary CM, et al. Characterization of methocel cellulose ethers by aqueous SEC with multiple detectors. Carbohydr Polym. 2001;45(3):293–303.
16. Cheng H, Wang Y, Hong Y, Wu F, Shen L, Lin X, et al. Low viscosity hydroxypropyl methylcellulose obtained by electron beam irradiation and its performance in spray drying. Int J Biol Macromol. 2024;275:133626.
17. Wang Y, Xie Y, Xu D, Lin X, Feng Y, Hong Y, et al. Hydroxypropyl methylcellulose reduces particle adhesion and improves recovery of herbal extracts during spray drying of Chinese herbal medicines. Dry Technol. 2014;32(5):557–566.
18. Cheng H, Wang Y, Hong Y, Wu F, Shen L, Lin X, et al. Low-viscosity hydroxypropyl methylcellulose obtained by electron beam irradiation and its performance in spray drying. Int J Biol Macromol. 2024;275:133626.
19. Wang L, Bu Y, Sun L, Chen H, et al. A sequential combination of advanced oxidation and enzymatic hydrolysis reduces the enzymatic dosage for lignocellulose degradation. Renew Energy. 2023;211:617–625.
20. Goodwin DJ, Picout DR, Ross-Murphy SB, Holland SJ, Martini LG, Lawrence MJ, et al. Ultrasonic degradation for molecular weight reduction of pharmaceutical cellulose ethers. Carbohydr Polym. 2011;83(2):843–851.
21. Schittenhelm N, Kulicke WM, et al. Producing homologous series of molar masses for establishing structure-property relationships with the aid of ultrasonic degradation. Macromol Chem Phys. 2000;201(15):1976–1984.
22. Camino NA, Pérez OE, Pilosof AM, et al. Molecular and functional modification of hydroxypropyl methylcellulose by high-intensity ultrasound. Food Hydrocoll. 2009;23(4):1089–1095.
23. Demappa T, Ganesha S, Divakara S, Pattabi M, Somashekar R, et al. Physical and thermal properties of 8 MeV electron beam irradiated HPMC polymer films. Nucl Instrum Methods Phys Res B. 2008;266(18):3975–3980.
24. Asha S, Demappa T, Sanjeev G, Parameswara P, Somashekar R, et al. Spectroscopic and thermal studies of 8 MeV electron beam irradiated HPMC films. Nucl Instrum Methods Phys Res B. 2009;267(14):2385–2389.

© STM Journals 2026. All Rights Reserved

25. Fei X, Jia W, Wang J, Chen T, Ling Y, et al. Study on enzymatic hydrolysis efficiency and physicochemical properties of cellulose and lignocellulose after pretreatment with electron beam irradiation. Int J Biol Macromol. 2020;145:733–739.
26. Dow Chemicals, et al. Handbook on Methocel Cellulose Ether Products. Dow Chemical; 1975. Archer WL, et al. Determination of Hansen solubility parameters for selected cellulose ether derivatives. Ind Eng Chem Res. 1991;30(10):2292–2298.
27. Yu LX, et al. Pharmaceutical quality by design: Product and process development, understanding and control. Pharm Res. 2008;25(4):781–791.
28. Andersson M, Wittgren B, Wahlund KG, et al. Ultrahigh molar mass component detected in ethyl hydroxyethyl cellulose by asymmetrical flow field-flow fractionation coupled to multiangle light scattering. Anal Chem. 2001;73(20):4852–4861.
29. Bos TS, Pirok BW, Karlson L, Schantz S, Dahlseid TA, Stoll DR, et al. Fingerprinting of hydroxy propyl methyl cellulose by comprehensive two-dimensional liquid chromatography-mass spectrometry of monomers resulting from acid hydrolysis. J Chromatogr A. 2024;1722:464874.
30. Sangappa B, Maheswarappa, Demappa, Thippaiah, Dasaiah, Mahadevaiah, et al. Physical and thermal properties of 8 MeV electron irradiated HPMC polymer films. Nucl Instrum Methods Phys Res B. 2008;266:3975–3980.
31. Li W, Buckton G, et al. Using DVS-NIR to assess the water sorption behavior and stability of a griseofulvin/PVP K30 solid dispersion. Int J Pharm. 2015;495(2):999–1004.
32. Baghel S, Cathcart H, O'Reilly NJ, et al. Theoretical and experimental investigation of drug-polymer interaction and miscibility and its impact on drug supersaturation in aqueous medium. Eur J Pharm Biopharm. 2016;107:16–31.
33. Punčochová K, Heng JY, Beránek J, Štepánek F, et al. Investigation of drug-polymer interaction in solid dispersions by vapour sorption methods. Int J Pharm. 2014;469(1):159–167.
34. R.W. Unwin. AnyCoat Brochure. Available from: https://rwunwin.co.uk/wp-content/uploads/2022/06/AnyCoat-Brochure.pdf
35. Yoo YJ, Um IC, et al. Examination of thermo-gelation behavior of HPMC and HEMC aqueous solutions using rheology. Korea-Aust Rheol J. 2013;25(2):67–75.
36. Bodvik R, Dedinaite A, Karlson L, Bergstrom M, Baverback P, Pedersen J, et al. Aggregation and network formation of aqueous methylcellulose and hydroxypropyl methylcellulose solutions. Colloids Surf A Physicochem Eng Asp. 2010;354(1–3):162–171.
37. Liu SQ, Joshi SC, Lam YC, Tam KC, et al. Thermoreversible gelation of hydroxypropyl methylcellulose in simulated body fluids. Carbohydr Polym. 2008;72(1):133.
38. Yoo YJ, Um IC, et al. Examination of thermo-gelation behavior of HPMC and HEMC aqueous solutions using rheology. Korea-Aust Rheol J. 2013;25(2):67–75.
39. Perez-Robles S, Carotenuto C, Minale M, et al. HPMC hydrogel formation mechanisms unveiled by the evaluation of the activation energy. Polymers (Basel). 2022;14(3):635.
40. Tan YT, Heng PW, Wan LS, et al. Mixed polymer coating for modified release from coated spheroids. Pharm Dev Technol. 1999;4(4):561–570.

© STM Journals 2026. All Rights Reserved